Nano-Structures & Nano-Objects 27 (2021) 100770

Contents lists available at ScienceDirect

Nano-Structures & Nano-Objects

journal homepage: www.elsevier.com/locate/nanoso

Tannin from *Schinopsis balansae* applied to the nanofunctionalization of protective antifungal coatings

Erasmo Gámez-Espinosa [a,*], Cecilia Deyá [a,b], Marta Cabello [c,d], Natalia Bellotti [a,d]

[a] Centro de Investigación y Desarrollo en Tecnología de Pinturas (CONICET-CICBA-Ing.-UNLP), Buenos Aires, Argentina
[b] Facultad de Ingeniería. Universidad Nacional de La Plata, Buenos Aires, Argentina
[c] Instituto de Botánica "Carlos Spegazzini"(CICPBA-UNLP), Buenos Aires, Argentina
[d] Facultad de Ciencias Naturales y Museo. Universidad Nacional de La Plata, Buenos Aires, Argentina

ARTICLE INFO

Article history:
Received 11 January 2021
Received in revised form 12 April 2021
Accepted 10 July 2021

Keywords:
Green silver nanoparticles
Fungal deterioration
Acrylic paint
Protective coatings

ABSTRACT

Fungal physical, chemical and aesthetical deterioration can occur by microbial biofilms adhere to the surface, leading to alterations on the paints integrity. The sol–gel method affords various merits and added with biocides can be used to control paint films biodeterioration. The aim of the present research was to obtain an efficient antifungal protection to waterborne paint films using a sol–gel coating added with silver nanoparticles synthesized by a green methodology using *Schinopsis balansae* tannin aqueous solution. Herein, was used a low cost and eco-friendly method for the preparation of silver nanoparticles. The antifungal activity was assessed against *Aspergillus niger* MN371276, *Penicillium commune* MN371392, *Cladosporium sphaerospermum* MN371394 and *Lasiodiplodia theobromae* MN371283. In addition, the nanofunctionalized antifungal coatings were characterized by SEM micrographs, EDS spectroscopy and mapping, contact angle and determination and absorption/ desorption cycles of humidity. Fungal resistance test of sol–gel coating silver nanoparticles over the paint showed to be efficient to prevent fungal biofilm development with 100% inhibition against all strains tested.

1. Introduction

Biodeterioration by microorganisms is predominately observed not only on items of cultural heritage, stone artifacts such as historical monuments but on modern materials, buildings and paints [1,2]. A typical example is biofilm formation of filamentous fungi on paints. Microbials adhere to painted surfaces affecting the aesthetic and the integrity of the films as they grow and spread on them [3,4]. Fungi are considered broadly versatile biodeteriogens, being able to thrive in materials and through their synergistic aesthetic, physical and chemical actions contribute to their biodeterioration [5–7]. Fungal biophysical biodeterioration can occur by the contraction and expansion of hyphae, leading to the breakdown of the paint film [8,9]. On the other hand, chemical biodeterioration occurs as a result of the action of exoenzymes and organic acids, leading to possible dissolution of the original components of the paint formulation [10,11]. Waterborne paints are specially molds target due to the use of water as solvent and the organic additives necessary to obtain a stable dispersed system [12]. In this sense, cellulosic thickeners are considered among the most susceptible of additives. Fungi are also known to interfere with paints aesthetical properties due to their high cell wall melanin contents and their contribution to inorganic pigments chromatic changes [13,14]. Therefore, it is imperative to implement efficient control strategies to preserve paints from fungal defacement.

A very powerful tool in obtaining nanomaterials is the use of photocatalysts. Related papers have been reported by different research groups. For example, Oveisi et al. 2010 [15] reported on a further simple and low-cost synthetic method and synthesized mesoporous titania films by utilizing bottom-up nanotechnology with surfactant assembly. In addition, the extraordinary antibacterial property of mesoporous titania films is discovered. The inactivation effect of bacteria is determined by several significant factors such as surface area, titania phase, anatase crystallinity, and surface morphology. Other authors propose a novel way to construct mesoporous architectures through evaporation-induced assembly of polymeric micelles with crystalline nanosheets that offer many advantages over commercial block copolymers [16]. Moreover, Bastakoti et al. 2014 [17], proposed the synthesis of mesoporous metal oxide materials with various compositions by assembly of spherical polymeric micelles consisting of triblock copolymer poly(styrene-b-2-vinyl pyridine-b-ethylene oxide) (PS-b-PVP-b-PEO) with three chemically distinct units. This approach is based on assembly of the stable micelles using a simple, highly reproducible method and

* Corresponding author.
E-mail addresses: e.gamez@cidepint.ing.unlp.edu.ar (E. Gámez-Espinosa), n.bellotti@cidepint.ing.unlp.edu.ar (N. Bellotti).

https://doi.org/10.1016/j.nanoso.2021.100770
2352-507X/

is widely applicable toward numerous compositions that are difficult for the formation of mesoporous structures.

Nevertheless, sol–gel coating added with eco-friendly biocides can be used against the fungal deterioration of paints. The sol–gel process involves the transition of a system from liquid phase (sol) to solid phase (gel) through chemical reactions of hydrolysis and condensation of the precursors [18]. The sol–gel method affords various merits as follows: reliability of the consuming equipment, simple fabrication environment, high uniformity on the thin films and utilization of different sizes with substrate combinations [19,20]. It has previously been observed that sol–gel coating added with biocides was used to control the biodeterioration of bricks [21]. Besides, coatings formulated with antimicrobials silica-additives obtained by the sol–gel method had antifungal activity against *Chaetomium globosum* and *Alternaria alternata* [22]. Antifungal activity of phytogenic synthesized silver nanoparticles (AgNPs) was well reported in the scientific literature [23–25]. In addition, this method is the preferred approach for the synthesis of metal and metal oxide nanoparticles due to its environmental friendliness, feasibility, and safety to human health when compared with other chemical or physical methods [26].

Schinopsis balansae commonly known as "quebracho colorado" is a native tree from South America and is very appreciated for its high content of tannins [27,28]. These tannins have been used for antifouling [29–31] and anticorrosive coatings [32]. Principal components of "quebracho" tannin (TQ) are polyphenols, easily extractable by hot water [30]. Polyphenols as those present in TQ possess antioxidant properties which could be attributed to their ability to donate hydrogens, electrons and chelate metal ions involved in generating free radicals. This turns out promising to the bio-reduction of metallic ions to obtain NPs with antimicrobial potential [33].

The aim of the present research was to obtain sol–gel coating functionalized with AgNPs obtained from *S. balansae* tannin aqueous solution to the control of waterborne paint fungal deterioration. Therefore, this work constitutes the first study reported on the use of a sol–gel coating functionalized with nano-additive phytosynthesized from "quebracho colorado" tannin and its antifungal performance in waterborne paint protective systems.

2. Materials and methods

2.1. Phytosynthesis and characterization of nanoparticles

The nanoparticles were obtained starting from an aqueous solution of $AgNO_3$ to which the TQ solution was added in constant agitation for 30 min at 60 °C and pH was adjusted to 7 by NH_4OH solution [34]. The final concentration of the salts in the synthesis system was 10^{-2} M. Two concentrations of TQ (UNITAN) were used: 500 and 1000 ppm. The particles in suspension were kept in the fridge at 4 °C in caramel flasks.

Firstly, UV–Vis spectroscopy was carried out to verify the presence of the NPs and then to assess their stability over time (1, 30, 60 and 90 days). The measurements were made in a UV SP 2000 spectrophotometer. Transmission Electron Microscopy (TEM) was applied to confirm the obtaining of the nanoparticles, observe their morphology and particle size. The equipment used was a JEOL 100 CXII at an acceleration voltage of 100 KV. The NPs were purified by successive washes using a microcentrifuge DLAB D3024R at 15 000 rpm during 20 min at 20 °C. Scanning electron microscopy (SEM), energy dispersive x-ray spectroscopy (EDS) and x-ray mapping were made to the purified NPs. The microscope was a Philips FEI Quanta 200, and the working condition was low vacuum (10^{-2} torr). FTIR spectra of the purified NPs were obtained using the KBr disk method by a Perkin-Elmer Spectrum One Spectrometer. The analysis of the spectra was carried out using the KnowItAll® Informatics System program, Version: 10.0.18362.

2.2. Antifungal activity of nanoparticles

The strains selected for this study were: *Aspergillus niger* MN371276, *Penicillium commune* MN371392, *Cladosporium sphaerospermum* MN371394 and *Lasiodiplodia theobromae* MN371283. They were isolated from biodeteriorated facade of the Cathedral of La Plata city (34°55′S, 57°57′O) in a previous research work [35]. The antifungal activity of the NPs suspensions was determined by two tests: agar diffusion method (Kirby-Bauer) and macrodilution assay [36].

In case of agar diffusion method, Petri dishes were prepared with 15 mL of Malt Agar Extract (MEA) inoculated. The suspension used counted with 10^5 spores/mL. Next, paper 6 mm diameter discs embedded in 6 μL of the NPs suspensions were placed on the corresponding solid medium. The negative control was physiological solution and as positive control, a quaternary ammonium salt (hexadecyl trimethyl ammonium bromide) aqueous solution (3 mg/mL) was used. The Petri dishes were incubated at 28 °C for 48 h. Diameters (D) of the inhibition zone were measured by an Electronic Digital Caliber. The antifungal activity was considered positive when $D \geq 6$ mm (active) and negative when $D < 6$ (not active).

For the macrodilution method, fungal growth was determined through the measurement of the colony diameters. MEA with different concentrations of NPs suspensions (10, 50 and 167 μg/mL) were placed in Petri dishes. As a control, NPs-free Petri dishes with MEA were used (0 μg/mL). Subsequently, the plates were inoculated in the center with 20 μL spore suspension (10^5 spores/mL) and incubated for 7 days at 28 °C. The test was carried out in triplicate. The colony diameter was measured with Electronic Digital Caliber.

2.3. Formulation, preparation and characterization of nanofunctionalized coatings

NPs functionalized sol–gel coating was prepared to be applied in the protection of acrylic paints for outdoor environments. The acrylic paint was specially prepared to the present research work and the formulation can be seen in Table 1. The paint was prepared in a high-speed disperser. In a first step distilled water with antifoaming (Q202, Diransa) and thickener (Cellosize 52000, Dow) agents were dispersed and then, pH-stabilizer agent (AMP-95, Angus) disperser agents (Diransa), suspended in water were added. Afterwards, the pigments were added one by one and finally a mixture of the acrylic-styrene resin (Thyosil 190, Diransa), coalescents (white spirit and butylglycol) and antifoaming agent were added.

The acrylic paint was characterized by dispersion degree (Hegman method), drying time (ASTM D1640) [37], covering hiding power (ASTM D344) [38] and washability test. Hegman method consists in drawing the liquid coating down a calibrated tapered groove varying in depth from 100 to 0 mm. The depth at which continuous groupings of particles or agglomerates protrude through the surface is taken as the dispersion degree. In washability test, the paint is applied to a black plastic panel that is scrubbing with a nylon brush immersed in water. The number of back-and-forth strokes (cycles) required to observe the black substrate by removing the paint is determined.

Finally, the paint was applied on glass slides to be treated then by the sol–gel coating. To the sol–gel coatings, 3-Aminopropyl triethoxysilane (AMEO) (Camsi-X, used as supplied) was used as

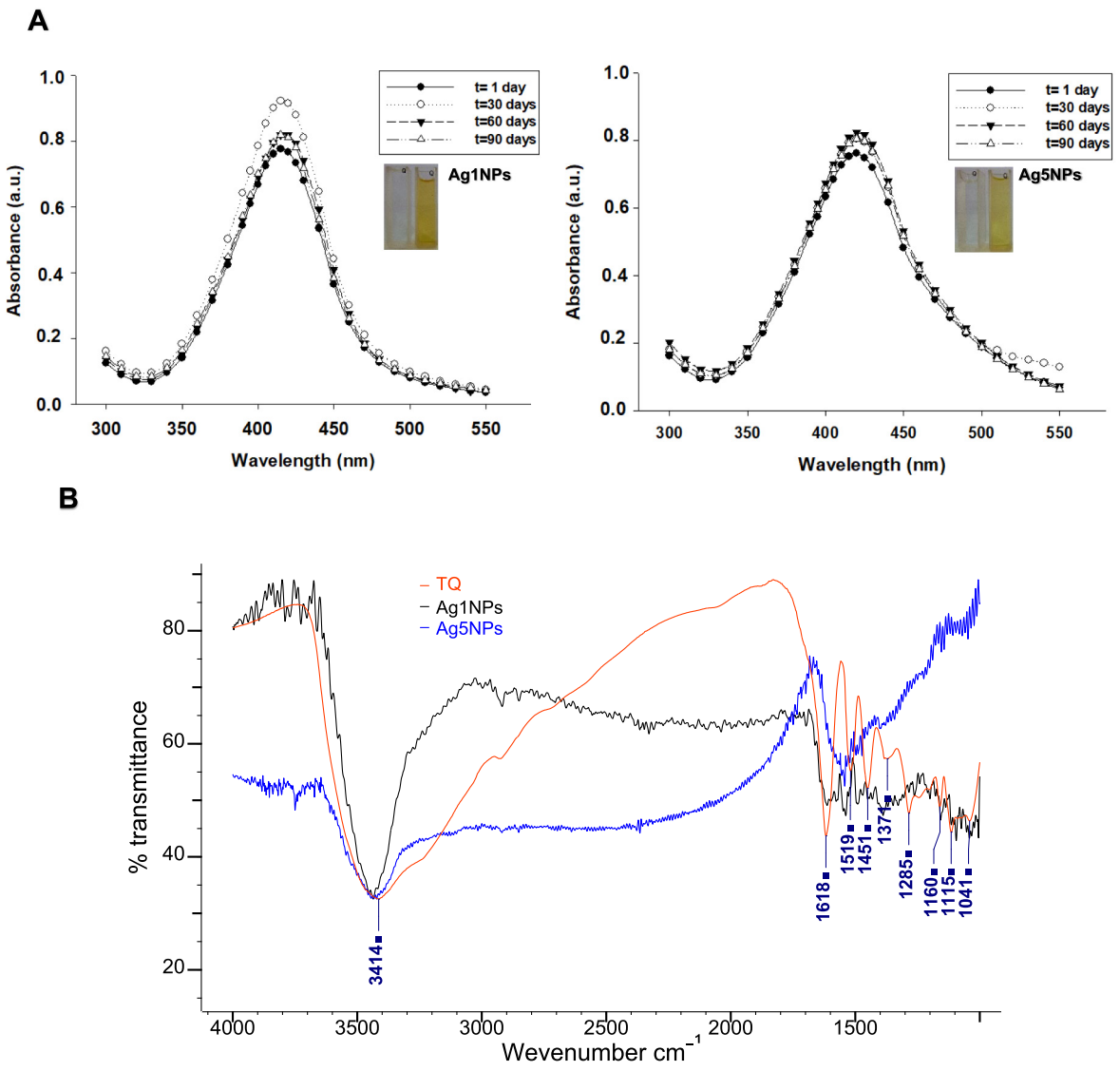

Fig. 1. UV–vis spectra (A) and FTIR spectra (B) of AgNPs synthesized with *S. balansae* tannin.

Table 1
Acrylic paint composition.

Compounds	% by weight
Water	16.40
Antifoaming agent	0.11
Thickener agent	0.22
pH-stabilizer agent	0.04
Disperser agents	0.15
Surfactant agent	0.04
TiO_2	9.96
Natural $CaCO_3$	21.91
Precipitated $CaCO_3$	1.95
Resin (1:1)	52.33
Coalescents	1.01

silane precursor and added in a concentration of 2% (v/v). The silane was added under constant stirring to a solution containing 0.9 mL/mL of ethanol, 0.06 mL/mL of NPs suspensions and distilled water (DW). The pH was previously adjusted to 4 with HNO_3. Controls, where the same volume of NPs in suspension was replaced by DW, were also prepared. After 1 h of hydrolysis, 2.5 cm^2 slide glasses with acrylic paint were immersed in the solutions for 90 s and allowed to dry for 14 days at 25 °C [21]. After this, the antifungal activity of the acrylic paint coated samples was evaluated.

The silane coatings were characterized by SEM, EDS, x-ray mapping, contact angles and absorption/desorption cycles of humidity. The contact angle was measured for triplicate by placing a drop of distilled water on the coated acrylic paint by a Pasteur pipette. A picture of the drop was taken by a Gaosuo digital microscope and the contact angle was measured by the Gaosuo software [39]. Dried coated glasses samples, previously weight in an analytical balance, were placed in a 100% humidity chamber and the gain of weight was determined during 1000 h in order to determine the water absorption/desorption. In every case, the assays were done in duplicate

2.4. Fungal resistance test of nanofunctionalized coatings

The antifungal activity of acrylic paint with the NPs-functionalized coatings, were evaluated using ASTM 5590 standard [40]. The samples were placed in Petri dishes with 10 mL of Minimum Mineral Agar (MMA). Each one was inoculated with the same volume (50 μL) of a spore solution (10^5 spores/mL). The fungal strains were the same as used before. Petri dishes were incubated at 28 °C for 30 days. The fungal growth observed in

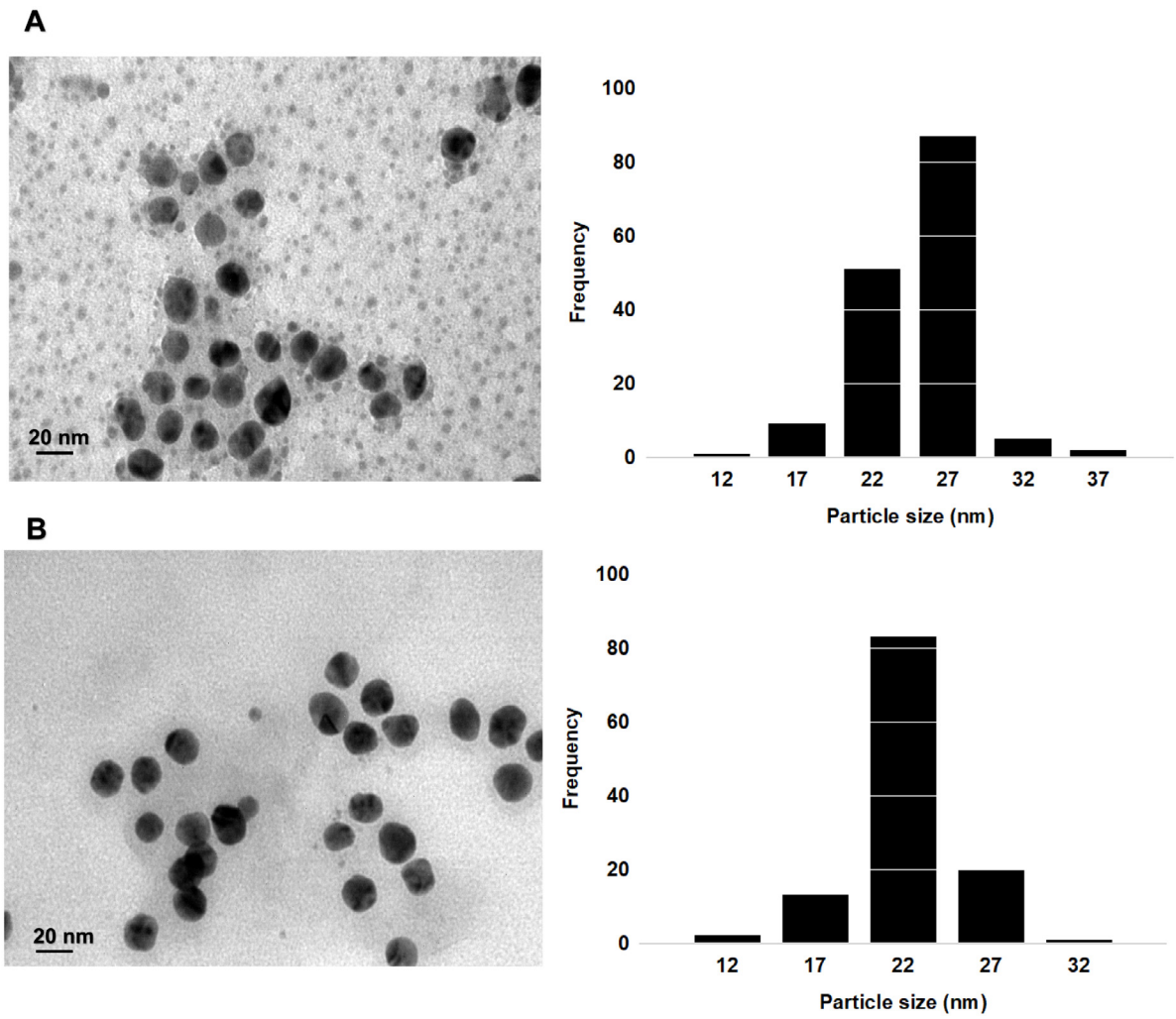

Fig. 2. TEM images (450000x) and histogram from size distribution analysis. A: Ag1NPs and B: Ag5NPs.

the samples was reported as the percentage (%) of the covered area (0%, <10%, 10%–30%, 30%–60% and 60%–100%) and classified as 1, 2, 3, and 4, respectively, taking into account the ASTM 5590 standard. At the end of the test, the samples were observed by stereoscopic microscope, Leica S8 APO, and photographic records were taken by Leica digital camera.

3. Result and discussion

3.1. Phytosynthesis and characterization of nanoparticles

With the proposed synthesis method, it was possible to obtain AgNPs. When TQ at 500 and 1000 ppm was added to the aqueous solution of $AgNO_3$, Ag5NPs and Ag1NPs were synthesized, respectively. This was evidenced in the UV–Vis spectra where the absorption band (~400 nm) corresponding to the surface plasmon resonance of the silver NPs could be observed [41]. Fig. 1 shows absorption UV–Vis spectra and FTIR spectra of AgNPs synthesized with TQ. Both UV–Vis spectra show maximum peaks approximately between 400 and 410 nm maintained over time, but increases in intensity for Ag1NPs only at 30 days (Fig. 1A).

On the other hand, in FTIR spectra of TQ and NPs obtained from TQ, there are well resolved peaks at 3414, 1618 and 1500–1000 cm^{-1} (Fig. 1B). Peaks between 3600–3400 cm^{-1} corresponding to the stretching of the O-H group (intramolecular H bonds, single bridge). Increases in the strength of H-bonds are accompanied by shifts to lower frequencies of the absorption bands due to O-H stretching vibration. In addition, it was detected the peak at 1618 cm^{-1} assigned to carbonyl groups stretching that could be present in this kind of polyphenol [31]. In the case of Ag5NPs this peak can be seen shifted at lower frequencies which could be attributed to electrical effects due to the release of electrons from carbonyl groups [42]. The electron donation would be related to the reduction of metal ions and the formation of nanoparticles. Nevertheless, peaks between 1500–1000 cm^{-1} are due to the stretching of C–C corresponds to phenols [31,43]. The presence of these functional groups in the purified Ag1NPs and Ag5NPs allows us to propose a biosynthesis mechanism: polyphenols present in the TQ would reduce the Ag^{+} ions to Ag°, acting as green reducing and stabilizer agent. Others studies have indicated that biomolecules like proteins, carbohydrates, flavonoids and phenols not only play a role in the capping of the nanoparticles, but also play an important role in reducing the ions to the nano size [26].

Fig. 2 illustrated the TEM images and histogram from size distribution analysis. Ag1NPs are quasi-spherical and showed higher frequency with an average size of 27 nm (Fig. 2A). In addition, Ag5NPs have the same shape that Ag1NPs but in this case the particles with lower average size (22 nm) were higher frequency (Fig. 2B). TEM images revealed that the particles are covered by a layer that would correspond with the tannins that could help to keep them stable and dispersed. Possibly, the morphology and

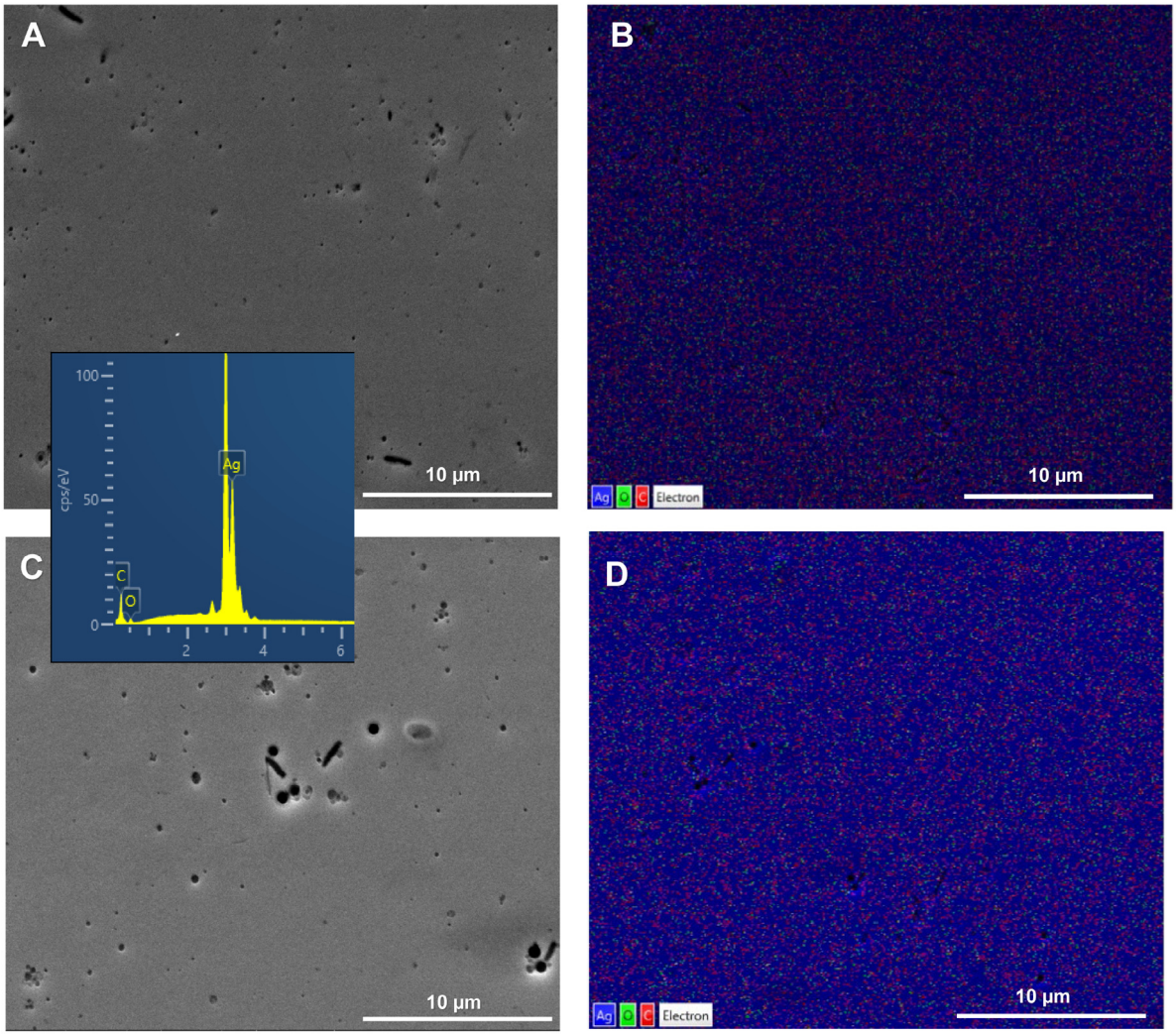

Fig. 3. SEM micrographs (10000x), Nps mapping and EDS spectra. A and B: Ag1NPs. C and D: Ag5NPs.

particle size were influenced by the reaction conditions such as the reactants concentration, type of the reducing agent (polyphenols) and synthesis time or temperature. Gámez-Espinosa et al. 2021 [44] have reported green synthesis of silver nanoparticles using *Caesalpinia spinosa* tannin. Interestingly, the average particle size in the present study (27 and 22 nm) using *S. balansae* was found big than the size of particles (15 and 7 nm) synthesized by *C. spinosa*. Similarly, the morphology is identical from nanoparticles synthesized by different tannins. By other side, Fig. 3 provides SEM micrographs, mapping and EDS spectra of biosynthesized NPs. The SEM image of Ag1NPs and Ag5NPs showed that the particles have a compact arrangement (Fig. 3A and C). EDS spectrum presented an Ag resolute peak at 3 keV, which clearly confirms the obtaining of AgNPs and reaffirms the results described by UV–Vis spectroscopy and TEM images. Finally, the mapping micrographs observed uniform distribution of AgNPs (Fig. 3B and D).

3.2. Antifungal activity of nanoparticles

Agar diffusion assay showed that Ag1NPs and Ag5NPs suspensions have antifungal activity on all the strains studied ($D \geq 6$ mm). For this reason, both NPs were used in the macrodilution assay. Fig. 4 shows the effect of NPs on fungal growth. Colony diameter values were higher when the strains faced Ag1NPs, even *A. niger* and *P. commune* grew when the concentration was 167 µg/mL. On the other hand, when the strains were faced with Ag5NPs, there was only growth from *A. niger* to 10 and 50 µg/mL and *P. commune* to 10 µg/mL (Fig. 4A). Therefore, Ag5NPs showed greater antifungal activity than Ag1NPs. This may be related to the difference in size since small nanoparticles have greater biological activity (27 and 22 nm for Ag1NPs and Ag5NPs respectively) [45]. In addition, *C. sphaerospermum* and *L. theobromae* are more sensitive to the biocide than *A. niger* and *P. commune*. Fig. 4B illustrated the macrodilution assay with the different concentrations of Ag5NPs in MEA against to the four strains at the end of the incubation period. Small colonies of *A. niger* and *P. commune* were observed when inoculated in medium with the lowest concentrations of NPs compared to control. On the other hand, there was no growth of *C. sphaerospermum* and *L. theobromae* in none of the concentrations of the Ag5NPs tested.

In the present study, the noteworthy antifungal activity was recorded from the biosynthesized AgNPs against four important deteriorating strains (*A. niger*, *P. commune*, *C. sphaerospermum* and *L. theobromae*) [35]. The AgNPs both reduced the mycelial growth of the tested fungi. Previously several scientists have reported the antifungal activity of AgNPs against different deteriorating fungi [21,36,46]. Recently, Scroccarello et al. 2021 [47] observed that the AgNPs synthesized using phenolic compounds exhibited antifungal activity against *A. niger*. However, the reports are lacking on the effect of AgNPs on *C. sphaerospermum*

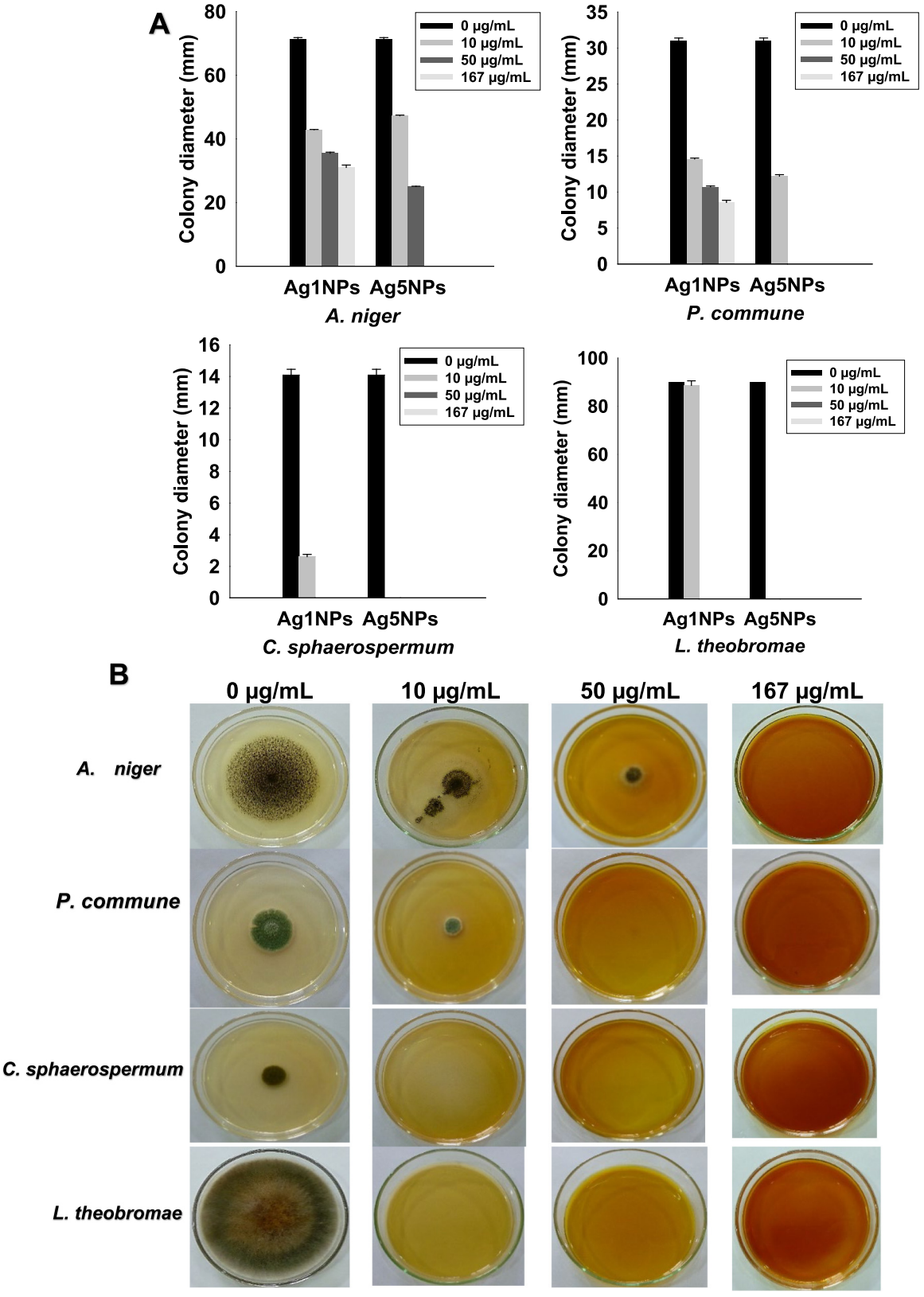

Fig. 4. Effect of NPs on the fungal growth. A: Colony diameter measurements. B: Macrodilution assay in Petri dish with MEA and Ag5NPs, $t = 7$ days, T = 28 °C.

As mentioned in the scientific literature a possible mechanism of antifungal activity is based on the internalization of AgNPs by the apical end of the growing hypha. Once the NPs are in the intracellular medium, their strong interaction with nucleophiles such as amino and thiol groups cause the inactivation of some enzymes and affect processes such as nutrition and cellular respiration. Silver ions can cause denaturation of proteins and DNA, which affects the replicative machinery in the fungal cell [23–25].

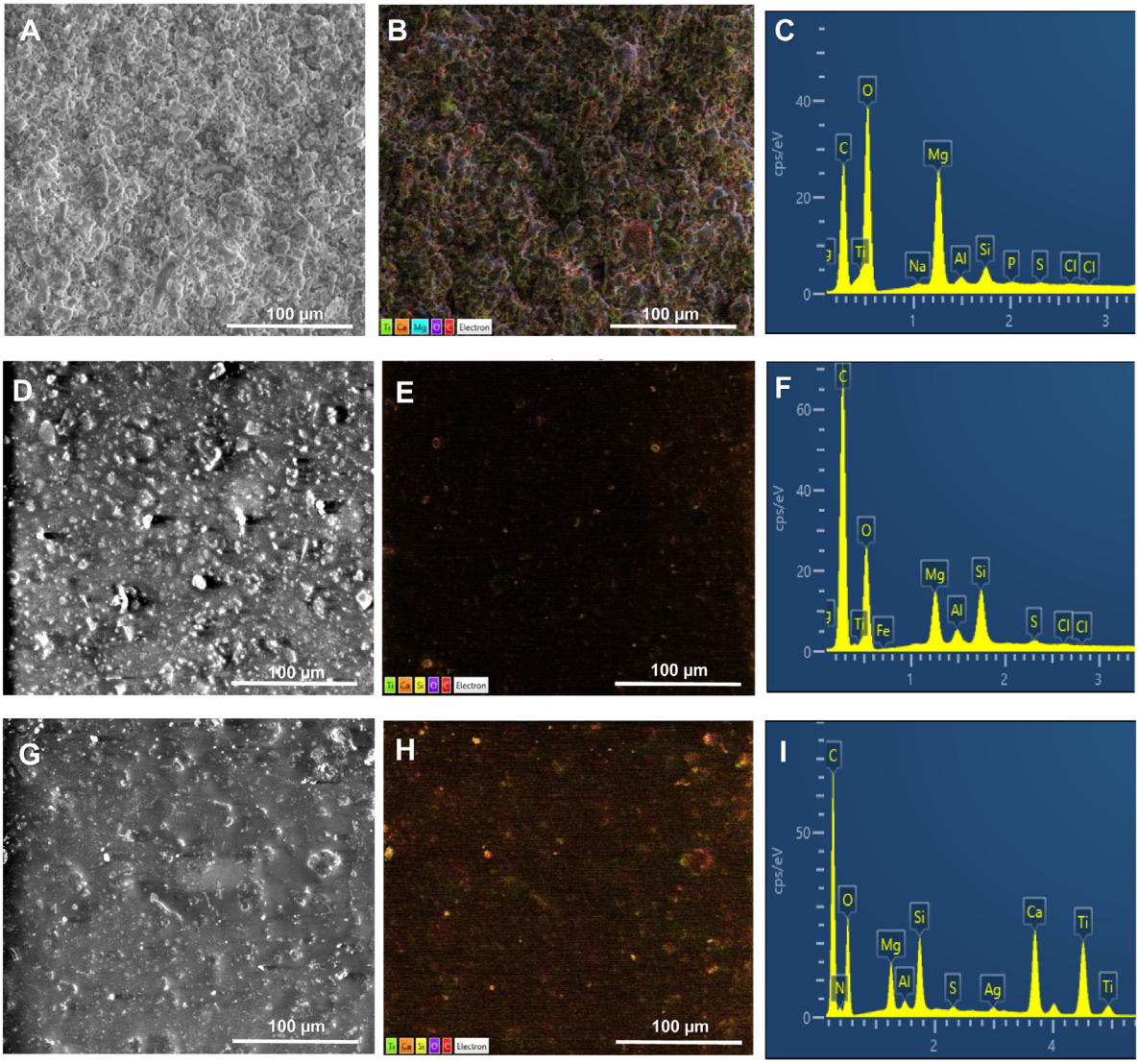

Fig. 5. SEM micrographs (1000x), x-ray mapping and EDS spectra. A-C: control (paint sol–gel free coating). D-F: Sol–gel coating over the paint. G-I: Sol–gel coating + Ag5NPs over the paint.

3.3. Formulation, preparation and characterization of nanofunctionalized coatings

Considering the absorption UV–Vis spectra, FTIR spectra, size distribution analysis and the antifungal activity, Ag5NPs suspension was selected as nano-additive to the formulation of the coatings. The proposed hydrolysis and condensation method allowed to obtain the sol–gel coating functionalized with Ag5NPs.

The characterization of the acrylic paint used was performed and the dispersion degree was over 100 µm, the set to touch was 45 min while the tough was 115 min. Hiding power was obtained after two cross applications (75+75 µm) and the washability was >4000 cycles. The values shown are acceptable for acrylic paint according to the standards used.

Fig. 5 illustrated SEM micrographs, x-ray mapping and EDS spectra of obtained coatings. Firstly, sol–gel coating free paint presents an irregular surface with a partially homogeneous distribution of elements such as Ti, Mg, O and C (Fig. 5A and B). Also, EDS spectrum peaks for these elements are observed at 0.4, 1.2, 0.5 and 0.1 keV, respectively (Fig. 5C). These elements are present in the chemical compounds used in the paint. The SEM figure of sol–gel coating and sol–gel coating + Ag5NPs over the acrylic paint presents a better homogenized surface, possibly due to the presence of the coating (Fig. 5D and G). In addition, x-ray mapping showed homogeneous distribution of elements such as Ti, Mg, O and C (Fig. 5E and H). The EDS spectra detected N and Si at 0.1 and 1.7 keV, respectively (Fig. 5F and I), these elements are part of the AMEO chemical structure used. A peak of Ag was observed at 3 keV in the EDS spectra of sol–gel coating + Ag5NPs over the paint. This would be indicating that the Ag5NPs were retained in the matrix during the drying of the sol–gel coating and they possibly interact with the amino groups of the silane [21,48].

Fig. 6 provides stereographs from water droplets on samples, the contact angle and absorption/desorption cycles of humidity. The contact angle values of paint sol–gel free coating, sol–gel coating over the paint and sol–gel coating + Ag5NPs over the paint were 70.0 ± 0.6°, 76.6 ± 0.7° and 84.2 ± 0.5°, respectively (Fig. 6A-C). Then, all samples were hydrophilic since the contact angle had values between 10° and 90° [39], however, the last Ag5NPs containing film is more hydrophobic than the others. The NPs in combination with adhesive is considered as a promising approach to fabricate mechanically durable hydrophobic surfaces on hard substrates by improving the adhesion between NPs component and the underlying substrates [49]. But, the sol–gel coating obtained not modified the hydrophobicity/hydrophilicity

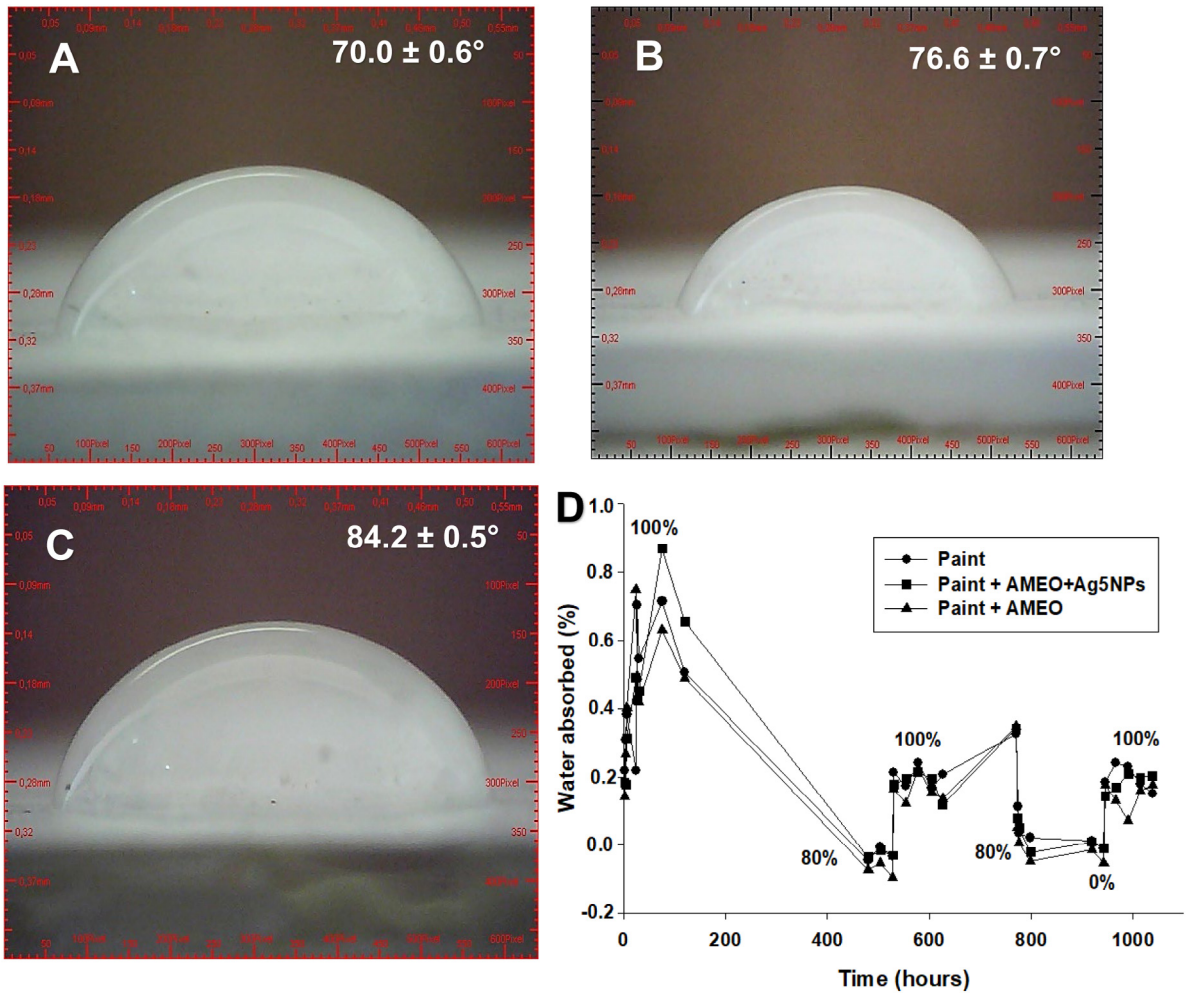

Fig. 6. Stereographs from water droplets on samples and the contact angle (A–C) and Absorption/desorption cycles of humidity (D). A: Paint sol–gel free coating, B: Sol–gel coating over the paint and C: Sol–gel coating + Ag5NPs over the paint.

characteristics of the acrylic paint. Scientific researches demonstrate that both rough micro/nanostructure and low surface energy components are indispensable for constructing hydrophobic surfaces [50]. However, due to the easily damaged or fragile feature of microscopic roughness, such extraordinary non-wetting textures are highly susceptible to mechanical destruction, even with moderate scratch (e.g. finger touch), which makes mechanical durability a major concern for hydrophobic surfaces in practical applications [51]. On the other hand, Fig. 6D showed there are no significant differences in humidity absorption between the acrylic paint with and without silane. In the first cycle, a lot of moisture is absorbed, then in the second and third it stabilizes at 0.2%. The desorption of water is similar. The glasses that are graphed are the ones that absorb the most for each sample. The results indicate that the presence of the silane film did not modified humidity absorption of the paint.

3.4. Fungal resistance test of nanofunctionalized coatings

It can be seen from the fungal growth rating according to the area covered in Table 2. The uncoated samples had heavy growth (60%–100%), except in the case of *P. commune* and *C. sphaerospermum* which had moderate growth (30%–60%) on acrylic paint. These fungal strains grew on the paint due to the presence of organic and inorganic compounds present in the formulation [2]. For example, organic compounds such as resin can serve as a carbon source. On the samples treated with the AMEO coating,

Table 2
Fungal growth rating according to the area covered.

Strains	Paint sol–gel free coating	Sol–gel coating over the paint	Sol–gel coating + Ag5NPs over the paint
A. niger	4	3	0
P. commune	3	2	0
C. sphaerospermum	3	2	0
L. theobromae	4	3	0

moderate growth of *A. niger* and *L. theobromae* was observed, although it was light (10%–30%) in the other two strains. However, there was no fungal growth on the samples when they were coated with AMEO + Ag5NPs due to the presence of NPs retained in the silane matrix [21,48].

Several authors have managed to functionalize sol–gel coating with nanoparticles applied to control corrosion and bacterial activity [52,53]. But much remains to be said about the use of sol–gel coatings with nanoparticles obtained by green synthesis applied as a protection system. One interesting finding is the obtention of functionalized sol–gel coating with AgNPs synthetized from *S. balansae* tannin for protection against fungal deterioration of acrylic paints. However, although this result is very promising, it is necessary to study the stability of the coating for more than 30 days and analyze the controlled release of Ag5Nps to optimize the formulation and extend the protective performance.

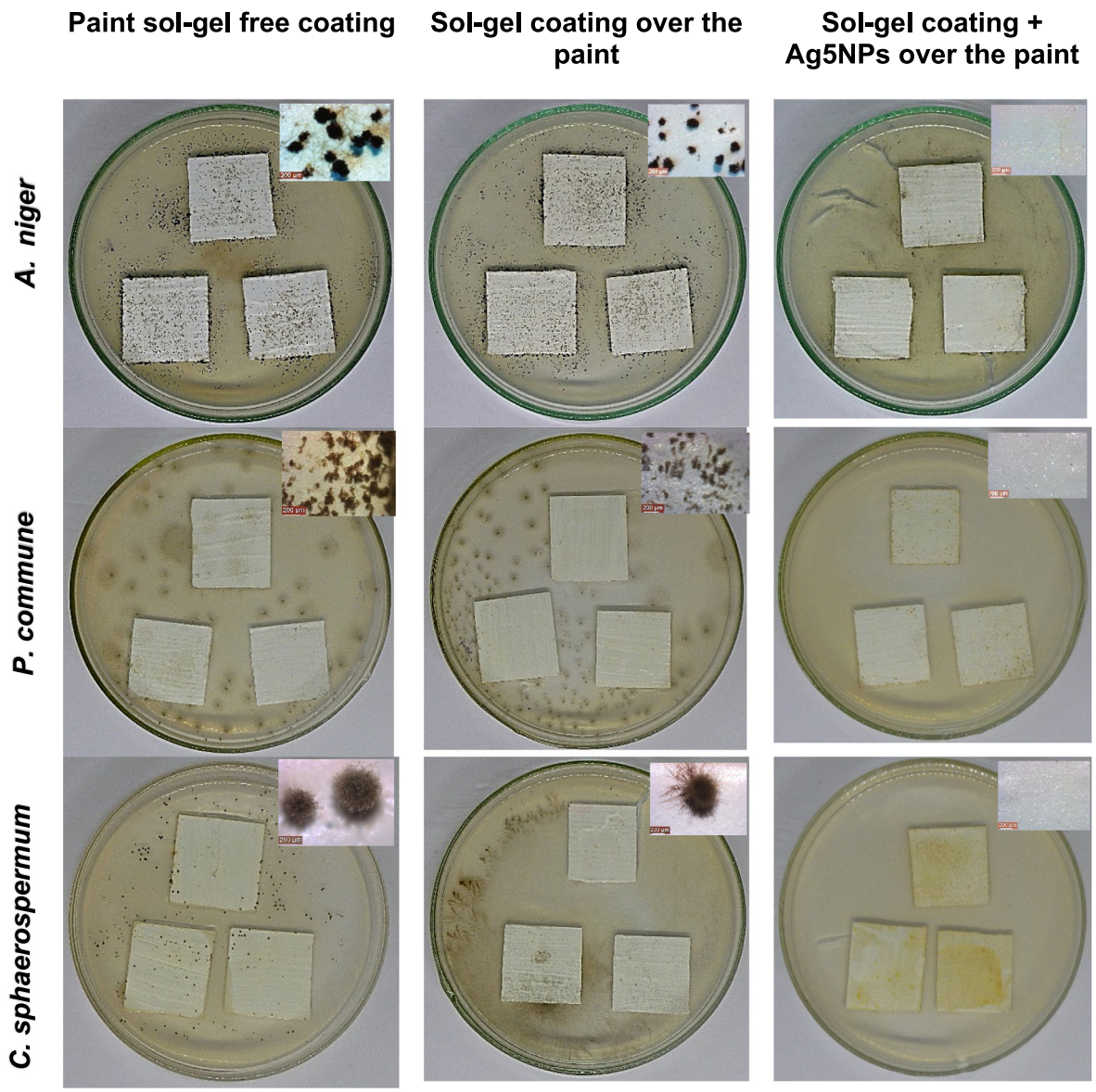

Fig. 7. Fungal resistance test against the strains, $t = 30$ days and T = 28 °C. Details were obtained from stereoscopic microscope (80×).

The resistance test results of the samples against *A. niger*, *P. commune* and *C. sphaerospermum* were depicted in Fig. 7. Both in paint without and with sol–gel coating, vegetative and reproductive mycelia were observed on the culture medium and on the samples. Instead, sol–gel coating + Ag5NPs over the paint showed to be efficient to prevent fungal biofilm development with 100% inhibition against strains. This evidence shows that the antifungal activity of the coating is related to the presence of Ag5NPs.

4. Conclusions

The synthesis of nanoparticles with antifungal activity from an aqueous solution of $AgNO_3$ and tannin from *S. balansae* was possible. Depending on the tannin concentration, the antifungal activity varies, being higher when tannin concentration is lower which is consistent with a smaller average size of the particles obtained.

Considering the antifungal activity and the properties studied by UV–Vis spectra, TEM, IR, SEM and EDS spectroscopy, the silver nanoparticles obtained with the lower tannin concentration was selected as nano-additive to the formulation of the coatings. UV–Vis spectra showed that the plasmon was more stable along time; IR spectra showed that polyphenols from quebracho tannin were involved in the synthesis and stabilization while by TEM NPs could be analyzed with Ag5NPs being smallest average size.

Sol–gel coating + Ag5NPs applied over the acrylic paint showed efficient to control fungal deterioration. The inhibition of the growth of *A. niger, P. commune*, *C. sphaerospermum* and *L. theobromae* was complete.

The inhibition of the growth due to sol–gel coating + Ag5NPs, could be due to the combination effect of the silver ions that interacts with enzymes affecting their function and the hydrophobic characteristic of the film.

In this sense, the application of silane coatings on painted materials is promising to extend their service life or increase the antimicrobial potential of the surfaces. These coatings could be used as a useful tool in the maintenance of paint films after a period of weathering.

CRediT authorship contribution statement

Erasmo Gámez-Espinosa: Methodology, Investigation, Writing - original draft. **Cecilia Deyá:** Conceptualization, Visualization, Methodology, Supervision. **Marta Cabello:** Visualization, Methodology, Supervision. **Natalia Bellotti:** Conceptualization, Methodology, Resources, Visualization, Project Administration, Writing - review & editing, Supervision, Funding acquisition.

Declaration of competing interest

The authors declare that they have no known competing financial interests or personal relationships that could have appeared to influence the work reported in this paper.

Acknowledgments

Authors are thankfulf or the essential support of: Consejo Nacional de Investigaciones Científicas y Técnicas (CONICET), Argentina, Comisión de Investigaciones Científicas de la provincia de Buenos Aires (CICPBA), Argentina, Agencia Nacional de Promoción Científica y Tecnológica (ANPCyT), Argentina and Universidad Nacional de La Plata (UNLP), Argentina. They also thank the technical support of the Ing. Pablo Bellotti, Ing. Pablo Seré, Lic. Claudio Cerruti, Ing. Mateo Paez and Tec. Diego Tunessi.

References

[1] T.M. Abdel Ghany, A.M. Omar, F.M. Elwkeel, M.A. Al Abboud, M.M. Alawlaqi, Fungal deterioration of limestone false-door monument, Heliyon 5 (2019) e02673, http://dx.doi.org/10.1016/j.heliyon.2019.e02673.
[2] C.C. Gaylarde, L.H.G. Morton, K. Loh, M.A. Shirakawa, Biodeterioration of external architectural paint films – A review, Int. Biodeterior. Biodegrad. 65 (2011) 1189–1198, http://dx.doi.org/10.1016/j.ibiod.2011.09.005.
[3] J.-D. Gu, Microbial biofilms, fouling, corrosion, and biodeterioration of materials, in: Handb. Environ. Degrad. Mater., third ed., Elsevier, 2018, pp. 273–298, http://dx.doi.org/10.1016/B978-0-323-52472-8.00014-9.
[4] S. Londhe, S. Patil, K. Krishnadas, A.M. Sawant, R.K. Yelchuri, V.G.R. Chada, Fungal diversity on decorative paints of India, Prog. Org. Coat. 135 (2019) 1–6, http://dx.doi.org/10.1016/j.porgcoat.2019.05.020.
[5] J. Trovão, F. Gil, L. Catarino, F. Soares, I. Tiago, A. Portugal, Analysis of fungal deterioration phenomena in the first Portuguese King tomb using a multi-analytical approach, Int. Biodeterior. Biodegrad. 149 (2020) 104933, http://dx.doi.org/10.1016/j.ibiod.2020.104933.
[6] E. Gallego-Cartagena, H. Morillas, M. Maguregui, K. Patiño Camelo, I. Marcaida, W. Morgado-Gamero, L.F.O. Silva, J.M. Madariaga, A comprehensive study of biofilms growing on the built heritage of a Caribbean industrial city in correlation with construction materials, Int. Biodeterior. Biodegrad. 147 (2020) 104874, http://dx.doi.org/10.1016/j.ibiod.2019.104874.
[7] G. Beata, The use of -omics tools for assessing biodeterioration of cultural heritage: A review, J. Cult. Herit. (2020) http://dx.doi.org/10.1016/j.culher.2020.03.006.
[8] W. Ma, F. Wu, T. Tian, D. He, Q. Zhang, J.-D. Gu, Y. Duan, D. Ma, W. Wang, H. Feng, Fungal diversity and its contribution to the biodeterioration of mural paintings in two 1700-year-old tombs of China, Int. Biodeterior. Biodegrad. 152 (2020) 104972, http://dx.doi.org/10.1016/j.ibiod.2020.104972.
[9] I.R. Abdel-Rahim, N.A. Nafady, M.M.K. Bagy, M.H. Abd-Alla, A.M. Abd-Alkader, Fungi-induced paint deterioration and air contamination in the assiut university hospital, Egypt, Indoor Built Environ. 28 (2019) 384–400, http://dx.doi.org/10.1177/1420326X18765256.
[10] D. Boniek, L. Bonadio, C. Santos de Abreu, A.F.B. dos Santos, M.A. de Resende Stoianoff, Fungal bioprospecting and antifungal treatment on a deteriorated Brazilian contemporary painting, Lett. Appl. Microbiol. 67 (2018) 337–342, http://dx.doi.org/10.1111/lam.13054.
[11] N. Unković, S. Erić, K. Šarić, M. Stupar, Ž. Savković, S. Stanković, O. Stanojević, I. Dimkić, J. Vukojević, M. Ljaljević Grbić, Biogenesis of secondary mycogenic minerals related to wall paintings deterioration process, Micron. 100 (2017) 1–9, http://dx.doi.org/10.1016/j.micron.2017.04.004.
[12] P. Dileep, S. Jacob, S.K. Narayanankutty, Functionalized nanosilica as an antimicrobial additive for waterborne paints, Prog. Org. Coat. 142 (2020) 105574, http://dx.doi.org/10.1016/j.porgcoat.2020.105574.
[13] T. Rosado, M. Gil, J. Mirão, A. Candeias, A.T. Caldeira, Darkening on lead-based pigments: Microbiological contribution, Color Res. Appl. 41 (2016) 294–298, http://dx.doi.org/10.1002/col.22014.
[14] R.J.B. Cordero, A. Casadevall, Functions of fungal melanin beyond virulence, Fungal Biol. Rev. 31 (2017) 99–112, http://dx.doi.org/10.1016/j.fbr.2016.12.003.
[15] H. Oveisi, S. Rahighi, X. Jiang, Y. Nemoto, A. Beitollahi, S. Wakatsuki, Y. Yamauchi, Unusual antibacterial property of mesoporous titania films: Drastic improvement by controlling surface area and crystallinity, Chem. - Asian J. 5 (2010) 1978–1983, http://dx.doi.org/10.1002/asia.201000351.
[16] B.P. Bastakoti, Y. Li, M. Imura, N. Miyamoto, T. Nakato, T. Sasaki, Y. Yamauchi, Polymeric micelle assembly with inorganic nanosheets for construction of mesoporous architectures with crystallized walls, Angew. Chem. Int. Ed. 54 (2015) 4222–4225, http://dx.doi.org/10.1002/anie.201410942.
[17] B.P. Bastakoti, S. Ishihara, S.-Y. Leo, K. Ariga, K.C.W. Wu, Y. Yamauchi, Polymeric micelle assembly for preparation of large-sized mesoporous metal oxides with various compositions, Langmuir 30 (2014) 651–659, http://dx.doi.org/10.1021/la403901x.
[18] I.A. Neacşu, A.I. Nicoară, O.R. Vasile, B.Ş. Vasile, Inorganic micro- and nanostructured implants for tissue engineering, in: Nanobiomaterials Hard Tissue Eng., Elsevier, 2016, pp. 271–295, http://dx.doi.org/10.1016/B978-0-323-42862-0.00009-2.
[19] G.V. Kaliyannan, S.V. Palanisamy, E.B. Priyanka, S. Thangavel, S. Sivaraj, R. Rathanasamy, Investigation on sol–gel based coatings application in energy sector – A review, Mater. Today Proc. (2020) http://dx.doi.org/10.1016/j.matpr.2020.03.484.
[20] C.A. Hernández-Barrios, J.A. Saavedra, S.L. Higuera, A.E. Coy, F. Viejo, Effect of cerium on the physicochemical and anticorrosive features of TEOS-GPTMS sol–gel coatings deposited on the AZ31 magnesium alloy, Surf. Interfaces 21 (2020) 100671, http://dx.doi.org/10.1016/j.surfin.2020.100671.
[21] E. Gámez-Espinosa, L. Barberia-Roque, O.F. Obidi, C. Deyá, N. Bellotti, Antifungal applications for nano-additives synthesized with a bio-based approach, Adv. Nat. Sci. Nanosci. Nanotechnol. 11 (2020) 015019, http://dx.doi.org/10.1088/2043-6254/ab790f.
[22] R. Arreche, N. Bellotti, C. Deyá, P. Vázquez, Assessment of waterborne coatings formulated with sol–gel/Ag related to fungal growth resistance, Prog. Org. Coat. 108 (2017) 36–43, http://dx.doi.org/10.1016/j.porgcoat.2017.04.007.
[23] B. Żarowska, T. Koźlecki, M. Piegza, K. Jaros-Koźlecka, M. Robak, New look on antifungal activity of silver nanoparticles (AgNPs), Polish J. Microbiol. 68 (2019) 515–525, http://dx.doi.org/10.33073/pjm-2019-051.
[24] T. Khan, A. Yasmin, H.E. Townley, An evaluation of the activity of biologically synthesized silver nanoparticles against bacteria, fungi and mammalian cell lines, Colloids Surf. B 194 (2020) 111156, http://dx.doi.org/10.1016/j.colsurfb.2020.111156.
[25] K. Kavitha, N. Vijaya, A. Krishnaveni, M. Arthanareeswari, S. Rajendran, A. Al-Hashem, A. Subramania, Nanomaterials for antifungal applications, in: Nanotoxicity, Elsevier, 2020, pp. 385–398, http://dx.doi.org/10.1016/B978-0-12-819943-5.00019-1.
[26] T. Jasrotia, S. Chaudhary, A. Kaushik, R. Kumar, G.R. Chaudhary, Green chemistry-assisted synthesis of biocompatible Ag, Cu, and Fe2O3 nanoparticles, Mater. Today Chem. 15 (2020) 100214, http://dx.doi.org/10.1016/j.mtchem.2019.100214.
[27] V.A. Marchesini, M.D. Nosetto, J. Houspanossian, E.G. Jobbágy, Contrasting hydrological seasonality with latitude in the South American Chaco: The roles of climate and vegetation activity, J. Hydrol. 587 (2020) 124933, http://dx.doi.org/10.1016/j.jhydrol.2020.124933.
[28] W. Streit, D. Fengel, Purified tannins from quebracho colorado, Phytochemistry 36 (1994) 481–484, http://dx.doi.org/10.1016/S0031-9422(00)97100-0.
[29] N. Bellotti, B. Del Amo, R. Romagnoli, Assessment of tannin antifouling coatings by scanning electron microscopy, Prog. Org. Coat. 77 (2014) 1400–1407, http://dx.doi.org/10.1016/j.porgcoat.2014.05.004.
[30] N. Bellotti, C. Deyá, B. del Amo, R. Romagnoli, Quebracho tannin derivative and boosters biocides for new antifouling formulations, J. Coat. Technol. Res. 9 (2012) 551–559, http://dx.doi.org/10.1007/s11998-012-9403-0.
[31] N. Bellotti, B. del Amo, R. Romagnoli, Quaternary ammonium "Tannate" for antifouling coatings, Ind. Eng. Chem. Res. 51 (2012) 16626–16632, http://dx.doi.org/10.1021/ie301524r.
[32] C. Byrne, G.J. Selmi, O. D'Alessandro, C. Deyá, Study of the anticorrosive properties of quebracho colorado extract and its use in a primer for aluminum1050, Prog. Org. Coat. 148 (2020) 105827, http://dx.doi.org/10.1016/j.porgcoat.2020.105827.
[33] S. Valsalam, P. Agastian, M.V. Arasu, N.A. Al-Dhabi, A.-K.M. Ghilan, K. Kaviyarasu, B. Ravindran, S.W. Chang, S. Arokiyaraj, Rapid biosynthesis and characterization of silver nanoparticles from the leaf extract of Tropaeolum majus L. and its enhanced in-vitro antibacterial, antifungal, antioxidant and anticancer properties, J. Photochem. Photobiol. B Biol. 191 (2019) 65–74, http://dx.doi.org/10.1016/j.jphotobiol.2018.12.010.
[34] C. Deyá, N. Bellotti, Biosynthesized silver nanoparticles to control fungal infections in indoor environments, Adv. Nat. Sci. Nanosci. Nanotechnol. 8 (2017) 025005, http://dx.doi.org/10.1088/2043-6254/aa6880.

[35] E. Gámez-Espinosa, N. Bellotti, C. Deyá, M. Cabello, Mycological studies as a tool to improve the control of building materials biodeterioration, J. Build. Eng. 32 (2020) 101738, http://dx.doi.org/10.1016/j.jobe.2020.101738.
[36] M.A. Fernández, L. Barberia Roque, E. Gámez Espinosa, C. Deyá, N. Bellotti, Organo-montmorillonite with biogenic compounds to be applied in antifungal coatings, Appl. Clay Sci. 184 (2020) http://dx.doi.org/10.1016/j.clay.2019.105369.
[37] ASTM D1640 Test Methods for Drying, Curing, or Film Formation of Organic Coatings at Room Temperature, ASTM International, American Society for Testing and Materials, West Conshohocken, PA, USA, 2003.
[38] ASTM D344 Test Method for Relative Dry Hiding Power of Paints by the Visual Evaluation of Brushouts, ASTM International, American Society for Testing and Materials, West Conshohocken, PA, USA, 2016.
[39] K. Koch, W. Barthlott, Superhydrophobic and superhydrophilic plant surfaces: An inspiration for biomimetic materials, Philos. Trans. R. Soc. A Math. Phys. Eng. Sci. 367 (2009) 1487–1509, http://dx.doi.org/10.1098/rsta.2009.0022.
[40] ASTM D5590 Standard Test Method for Determining the Resistance of Paint Films and Related Coatings to Fungal Defacement by Accelerated Four-Week Agar Plate Assay, ASTM International, West Conshohocken, PA, 2010.
[41] M. Ider, K. Abderrafi, A. Eddahbi, S. Ouaskit, A. Kassiba, Silver metallic nanoparticles with surface plasmon resonance: Synthesis and characterizations, J. Clust. Sci. 28 (2017) 1051–1069, http://dx.doi.org/10.1007/s10876-016-1080-1.
[42] N. Bellotti, B. Del Amo, R. Romagnoli, Tara tannin a natural product with antifouling coating application, Prog. Org. Coat. 74 (2012) 411–417, http://dx.doi.org/10.1016/j.porgcoat.2011.11.014.
[43] R. Morrison, R. Boyd, Organic Chemistry, fifth ed., Allyn & Bacon, Boston, Massachusetts, United States, 1990.
[44] E. Gámez-Espinosa, C. Deyá, M. Cabello, N. Bellotti, Nanoparticles synthesised from caesalpinia spinosa: assessment of the antifungal effects in protective systems, Adv. Nat. Sci. Nanosci. Nanotechnol. 12 (2021) 015001, http://dx.doi.org/10.1088/2043-6254/abdfc1.
[45] A.K. Mittal, Y. Chisti, U.C. Banerjee, Synthesis of metallic nanoparticles using plant extracts, Biotechnol. Adv. 31 (2013) 346–356, http://dx.doi.org/10.1016/j.biotechadv.2013.01.003.
[46] L. Barberia-Roque, E. Gámez-Espinosa, M. Viera, N. Bellotti, Assessment of three plant extracts to obtain silver nanoparticles as alternative additives to control biodeterioration of coatings, Int. Biodeterior. Biodegrad. 141 (2019) 52–61, http://dx.doi.org/10.1016/j.ibiod.2018.06.011.
[47] A. Scroccarello, B. Molina-Hernández, F. Della Pelle, J. Ciancetta, G. Ferraro, E. Fratini, L. Valbonetti, C. Chaves Copez, D. Compagnone, Effect of phenolic compounds-capped AgNPs on growth inhibition of Aspergillus niger, Colloids Surf. B 199 (2021) 111533, http://dx.doi.org/10.1016/j.colsurfb.2020.111533.
[48] P.R. Seré, W. Egli, A.R. Di Sarli, C. Deyá, Preparation and characterization of silanes films to protect electrogalvanized steel, J. Mater. Eng. Perform. 27 (2018) 1194–1202, http://dx.doi.org/10.1007/s11665-018-3178-0.
[49] J. Seyfi, S.H. Jafari, H.A. Khonakdar, G.M.M. Sadeghi, G. Zohuri, I. Hejazi, F. Simon, Fabrication of robust and thermally stable superhydrophobic nanocomposite coatings based on thermoplastic polyurethane and silica nanoparticles, Appl. Surf. Sci. 347 (2015) 224–230, http://dx.doi.org/10.1016/j.apsusc.2015.04.112.
[50] A.T. Buruiana, F. Sava, E. Matei, I. Zgura, M. Burdusel, C. Mihai, A. Velea, Simple and clean method for obtaining Sn nanoparticles for hydrophobic coatings, Mater. Lett. 278 (2020) 128419, http://dx.doi.org/10.1016/j.matlet.2020.128419.
[51] X.-F. Zhang, F. Jiang, R.-J. Chen, Y.-Q. Chen, J.-M. Hu, Robust superhydrophobic coatings prepared by cathodic electrophoresis of hydrophobic silica nanoparticles with the cationic resin as the adhesive for corrosion protection, Corros. Sci. 173 (2020) 108797, http://dx.doi.org/10.1016/j.corsci.2020.108797.
[52] S. Zhang, X. Liang, G.M. Gadd, Q. Zhao, A sol–gel based silver nanoparticle/polytetrafluorethylene (AgNP/PTFE) coating with enhanced antibacterial and anti-corrosive properties, Appl. Surf. Sci. 535 (2021) 147675, http://dx.doi.org/10.1016/j.apsusc.2020.147675.
[53] E.A. González, N. Leiva, N. Vejar, M. Sancy, M. Gulppi, M.I. Azócar, G. Gomez, L. Tamayo, X. Zhou, G.E. Thompson, M.A. Páez, Sol–gel coatings doped with encapsulated silver nanoparticles: inhibition of biocorrosion on 2024-T3 aluminum alloy promoted by pseudomonas aeruginosa, J. Mater. Res. Technol. 8 (2019) 1809–1818, http://dx.doi.org/10.1016/j.jmrt.2018.12.011.